Oblique roughness replication in strained SiGe/Si multilayers

V. Holý
Laboratory of Thin Films and Nanostructures, Department of Solid State Physics, Faculty of Science, Masaryk University, Kotlářská 2, 61137 Brno, Czech Republic

A. A. Darhuber, J. Stangl, and G. Bauer
Institut für Halbleiterphysik, Universität Linz, Altenbergerstraße 69, A-4040 Linz, Austria

J. Nützel and G. Abstreiter
Walter Schottky Institut, Technische Universität München, Am Coulombwall 2, D-85748 Garching, Germany
(Received 30 April 1997; revised manuscript received 24 November 1997)

The replication of the interface roughness in SiGe/Si multilayers grown on miscut Si(001) substrates has been studied by means of x-ray reflectivity reciprocal space mapping. The interface profiles were found to be highly correlated and the direction of the maximal replication was inclined with respect to the growth direction. This oblique replication is explained by the influence of the inhomogeneous strain distribution around step bunches. The formation of step bunches is described by a kinetic step-flow model based on the work by Tersoff *et al.* [Phys. Rev. Lett. **75**, 2730 (1995)]. We have generalized this model by taking into account local variations of the in-plane strain. The angle of obliqueness deduced from these calculations agrees very well with the experimental findings. [S0163-1829(98)08719-0]

I. INTRODUCTION

The interface roughness in heteroepitaxial multilayers is an important parameter for their electrical and optical performance.[1] The associated well width fluctuations broaden the distribution of subband energies and correspondingly the intersubband transition energies relevant, e.g., for SiGe-based multi-quantum-well infrared detectors.[2–4]

Commercially available Si(001) substrates usually have an unintentional miscut in the range of $0.2°-0.5°$, and the epitaxial growth in this case may be dominated by the flow of monolayer steps. I.e., if the growth conditions provide for sufficiently large surface diffusion lengths, the impinging adatoms are incorporated preferably at the step edges. This step-flow growth mode has been studied both experimentally and theoretically for a number of years.[5–14] Tersoff *et al.*[9] developed a microscopic theoretical model for the temporal evolution of the step distribution. According to this model, the lattice mismatch induces a tendency for the monolayer steps to group together and to form so-called step bunches. Consequently, the surface of a strained layer (e.g., SiGe on Si) exhibits a steplike modulation with flat terraces between the step bunches. Dependent on the growth and material parameters, the step bunches contain typically several tens of monolayer steps and the size of the terraces is up to about 1 μm.

In the case of pseudomorphic multilayers and superlattices, the experimental finding was that the interface profiles are highly correlated.[15–23] If the strained layer is overgrown with the substrate material again (e.g., Si on SiGe), the surface modulation decreases and, finally, for sufficiently thick Si layers, a comparably flat surface with a homogeneous distribution of monolayer steps results.[24,19] Therefore it is not the morphology which induces an interface correlation, but inhomogeneous strain fields caused by the step bunches are attributed as the basis of the oblique replication mechanism.

Oblique roughness replication in SiGe/Si multilayers on vicinal Si substrates has been reported previously by Phang *et al.*[19] and Headrick, Baribeau, and Strausser[20] and the corresponding angles χ were determined. Phang *et al.*[19] suggested that the oblique replication is related to the presence of step-bunch-associated strain fields, but to our knowledge no quantitative theoretical approach to this phenomenon has been made so far.

The one-dimensional step-flow model by Tersoff *et al.*[9] has been formulated for a single growing layer with a homogeneous strain. It does not take into account lateral strain inhomogeneities occurring in a strained multilayer with a terraced interface structure. In order to study the influence of these inhomogeneities, we have generalized this model assuming a localized increase of the in-plane strain. As we will demonstrate, this local strain inhomogeneity has a strong influence on the density of the monolayer steps in its vicinity. It leads to the formation of a step bunch at the position of the disturbance. Due to the asymmetric shape of a step bunch, the in-plane strain peaks not directly above the step-bunch position, but laterally displaced, which explains the oblique replication of the interface profiles.

For experimental support of the proposed relations, we have performed high resolution x-ray reflectivity reciprocal space mapping on Si/SiGe multilayers. The experimental value for the angle between the growth direction and the direction of the roughness replication is in good agreement with the theoretical predictions.

Section II contains the sample parameters, the experimental setup of the synchrotron measurements, and the acquired reciprocal space map. In Sec. III A, we briefly describe the step-flow model by Tersoff *et al.*,[9] in Sec. III B we present an analytical model for the strain fields around an overgrown step bunch taking into account the relaxation at the free sur-

 © 1998 The American Physical Society

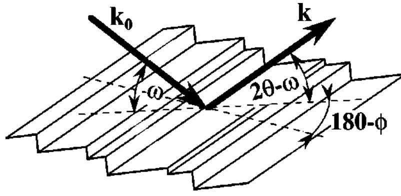

FIG. 1. Sketch of the scattering geometry. **k** and $\mathbf{k}_0$ are the primary and scattered x-ray wave vectors, respectively. ϕ describes the orientation of the scattering plane (determined by **k**, $\mathbf{k}_0$, and the surface normal) with respect to the miscut direction.

face. In Sec. III C, an inhomogeneous strain is incorporated into the step-flow model and the results are discussed in Sec. IV.

II. EXPERIMENT

SiGe/Si multilayer samples have been grown by solid source molecular beam epitaxy (MBE) at the Walter Schottky Institut using a Riber Siva 32 MBE.[25] In the following, we will concentrate on the results obtained on a ten period multi-quantum-well sample of nominally 30 Å $Si_{0.7}Ge_{0.3}$ and 151 Å Si on a nominally (001)-oriented Si substrate. The multi-quantum well was capped with nominally 270 Å Si. The growth temperature was varied between 500 °C for the SiGe wells and 400 °C for the Si barriers. The ramping of the temperature was done during the growth of the Si spacers.

The sample structure has been determined by high resolution x-ray diffraction and by subsequent analysis using dynamical diffraction theory. This yielded the following values for the layer thicknesses and the Ge concentration: Si-layer thickness $d_{\rm Si}=177$ Å, SiGe layer thickness $d_{\rm SiGe}=31$ Å, and Ge content $x_{\rm Ge}$ = 23%. The miscut angle β_0 has been determined by means of x-ray diffraction. We found $\beta_0=(0.51\pm0.01)°$; the azimuth of the miscut direction has been determined with an accuracy of $\pm5°$.

The specular and nonspecular x-ray reflection of the sample have been measured in a coplanar geometry at the OPTICS beamline of the European Synchrotron Radiation Facility (ESRF), Grenoble in a horizontal scattering geometry. A triple bounce Si (111) monochromator and a wavelength of 1.05 Å were used. The incidence angle of the x rays on the sample surface is called ω, while the deflection (scattering) angle is denoted as 2θ. By means of a narrow slit in front of the detector an angular resolution in 2θ of approximately 0.018° has been achieved. The divergence of the primary beam and hence the resolution in ω was about 0.002°. We have measured the distribution of the scattered intensity in reciprocal space (reciprocal space map) $I(\mathbf{Q})$, where $\mathbf{Q}=\mathbf{k}-\mathbf{k}_0$. **k** and $\mathbf{k}_0$ are the wave vectors of the incident and scattered beams, respectively. The Q_x axis is parallel to the sample surface and the Q_z axis is parallel to the outward surface normal. The angle ϕ determines the azimuthal orientation of the sample with respect to the incident x-ray beam (see Fig. 1).

From a fit of the specular reflectivity, the following values of the sample parameters were determined: the thicknesses of the individual layers: $d_{\rm Si}=(180\pm2)$ Å, $d_{\rm SiGe}=(26\pm2)$ Å, the root-mean-square (rms) roughness of the interfaces $\sigma=(7\pm1)$ Å, the thickness of the capping Si layer $d_{\rm cap}=(210\pm10)$ Å, thickness of the native oxide layer at the free surface $d_{\rm ox}=(30\pm15)$ Å.

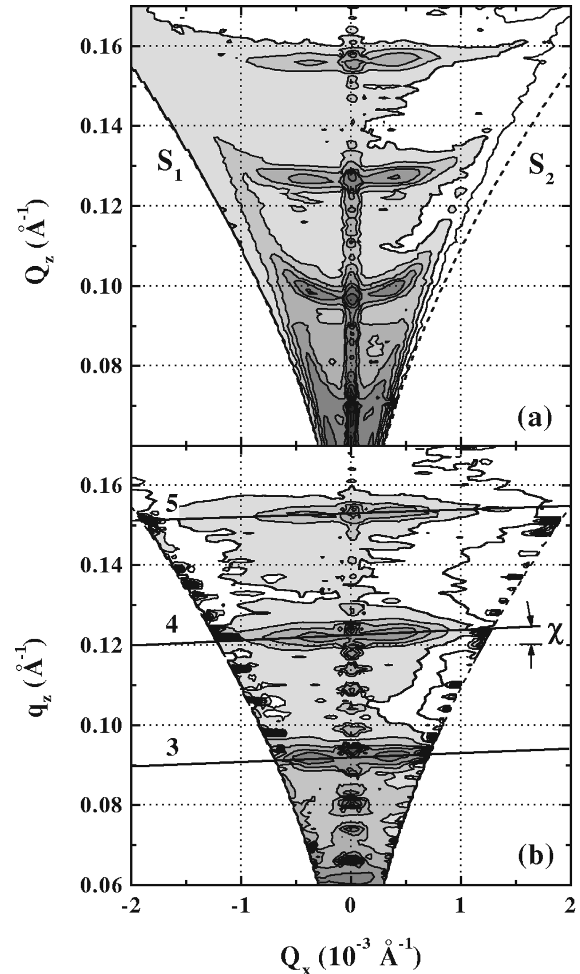

FIG. 2. Measured reciprocal space maps for $\phi=0°$ before (a) and after (b) the refraction correction. S_1 and S_2 label the margin of the accessible region of reciprocal space in the used coplanar scattering geometry. The RDS stripes are not parallel to the Q_x axis. Due to the large difference in the scales of the Q_x and the Q_z axes, the angle χ is distorted and seems to be smaller.

Since the ratio of the layer thicknesses in the multilayer is approximately 1:7, every eighth superlattice satellite should be suppressed. This occurs only if the reflectivities of both the Si-SiGe and SiGe-Si interfaces are similar. In the experimental reflectivity curve, the eighth satellite was close to, whereas the ninth and the subsequent satellites were well above, the background level. Therefore the rms roughnesses of the two interface types could differ by 1 Å at most. From a fit of 2θ scans, the vertical correlation length was determined as (2000 ± 500) Å,[23] i.e., the interface profiles are highly correlated throughout the entire multilayer stack.

In Fig. 2(a) we present a reciprocal space map of the scattered intensity measured for the azimuthal orientation $\phi=0$. In addition to the specular peaks at $Q_x=0$ we observe stripes of diffusely scattered intensity [so-called resonant diffuse scattering (RDS)] (Refs. 26 and 27) crossing the specular peaks. These stripes are not straight due to refraction of x rays at the sample surface. In Fig. 2(b), we have eliminated this refraction effect, which allows a more precise determi-

nation of the angle χ between the RDS stripes and the Q_x axis. The ordinate label q_z refers to the reciprocal space coordinate system after the refraction correction. χ equals the angle between the growth direction and the direction of maximal correlation of the interface profiles. If χ is zero, the replication direction is parallel to the growth direction. In the measurement presented in Fig. 2, χ is approximately 35° with an uncertainty of about 10°. This large value induces a pronounced asymmetry in ω scans, the trajectory of which is nearly parallel to the Q_x axis.[23] In the perpendicular sample orientation $\phi=90°$, the corresponding ω scans are symmetric and do not exhibit diffuse satellite peaks.[23] This ensures that the observed phenomenon is entirely related to the miscut of the sample.

We have measured reciprocal space maps around the third RDS maximum both for $\phi=0°$ and $\phi=180°$. As anticipated, the intensity asymmetry and the inclination of the RDS stripes measured in these two azimuthal orientations are opposite.

III. THEORETICAL DESCRIPTION

A. Step-flow model

The step-flow model describes the epitaxial growth process as a movement of individual monolayer steps at a strained vicinal surface. Tersoff *et al.*[9] provided equations of motion for the monolayer steps regarding both the interaction of the steps and the relevant growth parameters. The interaction of the monolayer steps is of elastic nature both with a repulsive and an attractive component.[28,29]

The force corresponding to the repulsive interaction between two steps at positions x and x' is given by $\alpha_2(x-x')^{-3}$ where α_2 is determined by the elastic constants and the surface energy.[28] The attractive force $\alpha_1(x-x')^{-1}$ depends on the strain in the system and is inversely proportional to the distance between two steps.[9] The following equation for the velocity v_m of the mth monolayer step has been derived:[9]

$$v_m=F\frac{x_{m+1}-x_{m-1}}{2}-B\left(\frac{f_{m+1}-f_m}{x_{m+1}-x_m}-\frac{f_{m-1}-f_m}{x_{m-1}-x_m}\right), \quad (1)$$

where B depends on the surface diffusion coefficient, the growth temperature, and the activation energy for the dissociation of an atom from a step. F is the flux rate per lattice site and f_m is the total force on a monolayer step with position x_m, which includes the interactions with all other steps in the system.

A numerical solution of this equation yielded the interesting result that the monolayer steps gather in groups (''bunches'') and atomically flat terraces exist between them. Since one step bunch can contain several tens of monolayer steps, a statistically significant description of the growth process requires the consideration of several thousands of individual monolayer steps. As such calculations would be very time consuming, we introduced a continuum description of the problem based on a step density $\rho(x,t)$, which corresponds to the inverse distance between neighboring steps.

Within the continuum approach, Eq. (1) can be rewritten as

$$v_m=\frac{F}{\rho(x_m)}-\frac{B}{\rho(x_m)}\left.\frac{\partial^2 f}{\partial x^2}\right|_{x_m}. \quad (2)$$

The force acting on the step at position x is

$$f(x)=\int_{-\infty}^{\infty}dx'\rho(x')\left[\frac{\alpha_1}{x-x'}-\frac{\alpha_2}{(x-x')^3}\right]. \quad (3)$$

Simple geometrical considerations yield the following relation between the step density and the step velocity:

$$\frac{\partial v}{\partial x}=-\frac{1}{\rho}\frac{\partial \rho}{\partial t}. \quad (4)$$

Inserting Eqs. (3) and (4) into Eq. (2) we obtain after some algebra the final equation

$$\frac{\partial \rho}{\partial t}=\frac{F}{\rho}\frac{\partial \rho}{\partial x}-B\left[\frac{1}{\rho}\frac{\partial \rho}{\partial x}\rho * G-\rho * G'\right], \quad (5)$$

where

$$G(x-x')=\frac{2\alpha_1}{(x-x')^3}-\frac{12\alpha_2}{(x-x')^5}$$

and G' is its first derivative; * denotes convolution. In replacing the discrete distribution of monolayer steps by a continuous one, a convergence of the integrals occurring in Eq. (5) can be achieved by introduction of a (small) cutoff radius R_0. For the qualitative behavior of the step-flow model its value is insignificant and we have chosen R_0 equal to the lattice constant. For the solution of Eq. (5) we have assumed periodical boundary conditions. The initial density distribution $\rho(x,t=0)$ is random with a mean value $\langle\rho(x,t=0)\rangle=\beta_0/h_0$, where β_0 is the miscut angle and h_0 is the height of the monolayer step.

Exact numerical values of the constants B and $\alpha_{1,2}$ are not known. α_1 can be approximated by $\alpha_1\approx\epsilon_{xx}^2 M h_0^2$, where M is the elastic constant and ϵ_{xx} is the strain in the growing layer.[9] The value of α_2 follows from the energetically most favorable separation $L_0=\sqrt{(\alpha_2/\alpha_1)}$ of an isolated step pair; we have used $L_0=10$ Å in our calculations. Only the order of the magnitude of B can be determined. If we assume that the surface diffusivity is sufficiently high so that every atom can reach the nearest monolayer step, we find $B\alpha_1\approx2\times10^5$ Å^3 s^{-1}.

In Fig. 3(a) we plotted the simulated function $\rho(x,t=40s)$ for three different fluxes F. It can be seen that sharp maxima of ρ occur for small F, while the modulation of the step density is shallower for large F. Therefore high and steep step bunches are formed for small F, while a large flux gives rise to a smoother interface profile [Figs. 3(b)–3(d)], where the angle between the terraces and the mean surface β is smaller than the nominal miscut β_0.

B. Deformation field of an interface containing step bunches

In a strained SiGe/Si multilayer with perfectly flat interfaces, the strain is confined to the strained SiGe layers only and it does not extend into the unstrained Si layers. If the interfaces of the SiGe layers are rough, inhomogeneous elas-

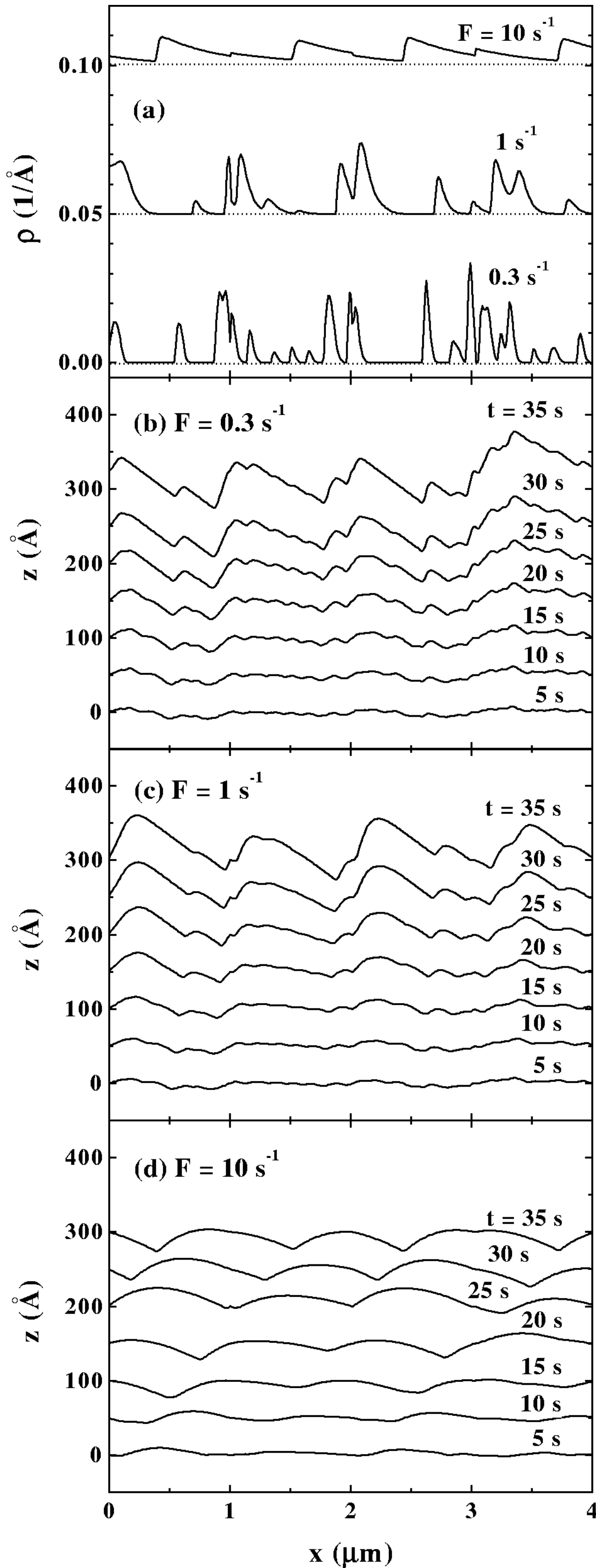

FIG. 3. (a) The step density ρ calculated for different flux rates F; (b)–(d) the temporal evolution of the surface profile of a single strained layer for various values of F. The profile is considerably smoother for large values of F (c) and no atomically flat terraces appear as in the case of small F. The vertical shift of the calculated surface profiles does not correspond to the actual shift of the surface during the growth which must be proportional to the flux F.

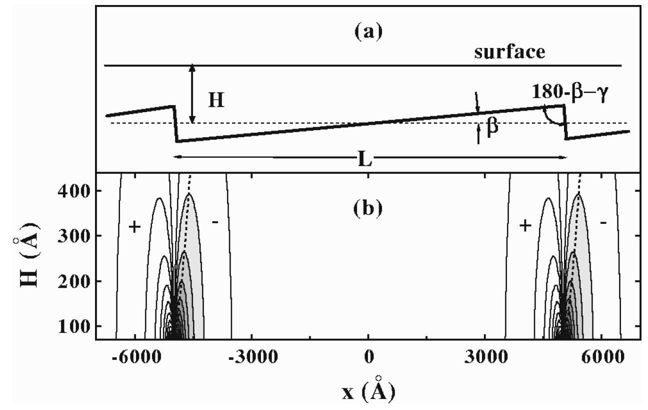

FIG. 4. (a) Sketch of the step-bunch geometry. H is the average Si-layer thickness, L is the average terrace width, and β is the miscut angle. (b) The dependence of the in-plane strain on the lateral position x and the average thickness of the Si-cap layer H. The dashed lines trace the local minima of the in-plane strain. The plus and minus signs label the regions of positive and negative in-plane strain, respectively.

tic strain fields extend into the Si layers, too. Thus, in the case of the step-flow growth, the deformation field originating in one SiGe layer affects the morphology of the subsequently grown SiGe layers.

In this section we outline the calculation of the strain field of a series of overgrown step bunches. The calculation is based on the elastic Green function[30] taking surface relaxation into account. This approach assumes elastic isotropy and identical elastic constants of both constituents (Si and SiGe). We assume straight steps parallel to the y axis, the x and z axes are parallel and perpendicular to the surface. The averaged SiGe-Si interface is parallel to the surface in depth H [Fig. 4(a)].

For the model calculations, the layer profile is replaced by a periodic series of steps with identical triangular cross section. The component ϵ_{xx} of the strain tensor at the free surface $z=0$ is

$$\epsilon_{xx}(x)=2\delta\frac{1+\nu}{\pi}\int_{-\infty}^{\infty}dx'\left[\frac{H-h(x')}{(x-x')^2+[H-h(x')]^2}-\frac{H}{(x-x')^2+H^2}\right]. \tag{6}$$

$h(x)$ describes the shape of the interface according to Fig. 4(a), δ is the lattice mismatch between SiGe and Si, and ν is the Poisson ratio. The assumed profile of the interface is sketched in Fig. 4(a). It is characterized by the angles β and γ and the base width L of the triangles. After simple but lengthy algebra Eq. (6) results in the expression

$$\epsilon_{xx}(x)=\sum_{n=-\infty}^{\infty}\epsilon_{xx}^{(t)}(x-nL), \tag{7}$$

where

$$\epsilon_{xx}^{(t)}(x)=2\delta\frac{1+\nu}{\pi}[\mathcal{F}(\beta,x+L/2,x_0+L/2,H)-\mathcal{F}(\beta,x+L/2,0,H)+\mathcal{F}(\gamma,x-L/2,0,H)-\mathcal{F}(\gamma,x-L/2,x_0-L/2,H)] \quad (8)$$

is the contribution of a single triangle. The function $\mathcal{F}$ is given by

$$\mathcal{F}(\beta,x,t,H)=\arctan\left(\frac{x-t}{H}\right)+\frac{\cos^2\beta}{2}\left\{2\arctan\left(\frac{x+H\tan\beta-t/\cos^2\beta}{x\tan\beta-h}\right)-\tan\beta\,\ln[(x-t)^2+(H-t\tan\beta)^2]\right\}. \quad (9)$$

In Fig. 4(b) we have plotted the dependence of the in-plane strain ϵ_{xx} at the surface as a function of x and H for the profiled defined by $L=1$ μm, $\beta=1°$, $\gamma=90°-\beta=89°$. The inhomogeneity of the strain distribution is clearly visible, the regions where $\epsilon_{xx}<0$ are shifted laterally with respect to the step-bunch positions in positive x direction, i.e., ''downstairs.'' The dotted lines in the figure mark the positions of the minima of ϵ_{xx} as a function of H. The result for $\gamma=80°$ is nearly identical, therefore its value is rather insignificant as long as it is much larger than β.

C. Roughness replication

In the preceding section we have shown that the step bunches on the interface of a strained SiGe layer induce inhomogeneous elastic strain fields in the unstrained Si layer above. The growth of the subsequent strained layer is affected by this inhomogeneous strain distribution, which superimposes on the homogeneous strain $\epsilon_{xx}^{(0)}$ due to the lattice mismatch. Since $a_{\mathrm{SiGe}}>a_{\mathrm{Si}}$, $\epsilon_{xx}^{(0)}$ is negative. Therefore at the point on the growing interface where ϵ_{xx} has a minimum, the value $|\epsilon_{xx}+\epsilon_{xx}^{(0)}|$ has a local maximum.

As shown in Refs. 28 and 9, the coefficient α_1 of the attractive force is proportional to the square of the in-plane strain. Therefore, in order to study the influence of inhomogeneous strain on the step-bunching mechanism, we add a term

$$\Delta\alpha_1=\alpha_1\left(1+\frac{\epsilon_{xx}}{\epsilon_{xx}^{(0)}}\right)^2-\alpha_1 \quad (10)$$

to the constant α_1 in Eq. (5). Inserting this expression into Eqs. (2) and (3) we obtain

$$\frac{\partial\rho}{\partial t}=\left(\frac{\partial\rho}{\partial t}\right)_{id}-B\Pi(x)\int_{-\infty}^{\infty}dx'\Pi(x')\rho(x')\Delta\alpha_1\times\left[\frac{1}{\rho(x)}\frac{\partial\rho(x)}{\partial x}\frac{2}{(x-x')^3}+\frac{6}{(x-x')^4}\right], \quad (11)$$

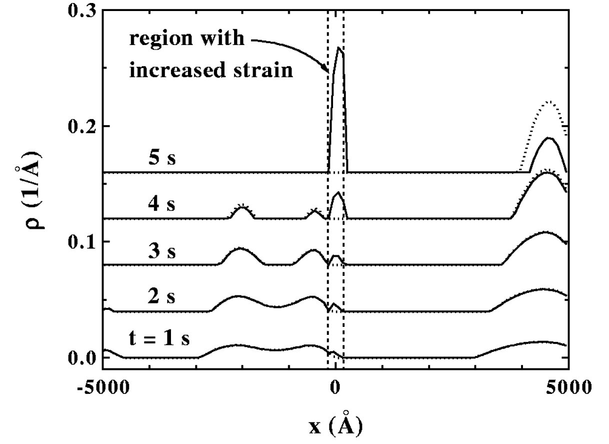

FIG. 5. The step density ρ without (dotted line) and with (full line) consideration of a local increase of α_1 by 10%.

where $(\partial\rho/\partial t)_{id}$ is the right-hand side of Eq. (5) and $\Pi(x)$ is the ''shape'' function of the disturbance (it equals unity in the region of increased strain and zero outside of it). After some algebra, we find

$$\frac{\partial\rho}{\partial t}=\frac{F}{\rho}\frac{\partial\rho}{\partial x}-B\left[\frac{1}{\rho}\frac{\partial\rho}{\partial x}\rho*G-\rho*G'\right]-4B\Pi(x)\rho(x_0)\Delta\alpha_1/R_0^3 \quad (12)$$

as the final equation. R_0 is the cutoff radius defined in Sec. III A. For the derivation of Eq. (12), we have assumed that an increased strain occurs only in a small region $x\in(x_0-l/2,x_0+l/2)$ and that the step density distribution $\rho(x,t)$ in this interval can be replaced by its value in the center $\rho(x_0,t)$. Moreover, we assumed $\Delta\alpha_1$ to be constant in this region.

In Fig. 5 we have plotted the resulting temporal evolution of the step density $\rho(x)$ calculated without (dashed line) and with (full line) the region of increased α_1. We used the values $\Delta\alpha_1/\alpha_1=0.1$ and $l=400$ Å. The other parameters were identical to the set used in Fig. 3. From the calculation follows that a local increase in the parameter α_1 results in a maximum of the step density corresponding to a step bunch. The physical interpretation of this effect is that the elastic strain relaxation in the step bunches decreases the total elastic energy stored in the strained layer. Therefore it is energetically favorable for a step bunch to form in the position of increased elastic energy density.

The obliqueness of the interface correlation is therefore caused by the asymmetry in the distribution of the elastic strain produced due to the asymmetrical interface profile. The obliqueness angle χ between the growth direction and the direction of the interface replication can be calculated from the shift of the minimum of the inhomogeneous strain ϵ_{xx} at the surface with respect to the position of the step bunch. In Fig. 6(a) we have plotted the dependence of χ on the depth of the interface H (which corresponds to the Si layer thickness) for different angles β between the terrace and the mean surface and a constant average distance $L=1.3$ μm between the step bunches. Figure 6(b) shows the dependence of χ on L for a constant $\beta=0.5°$.

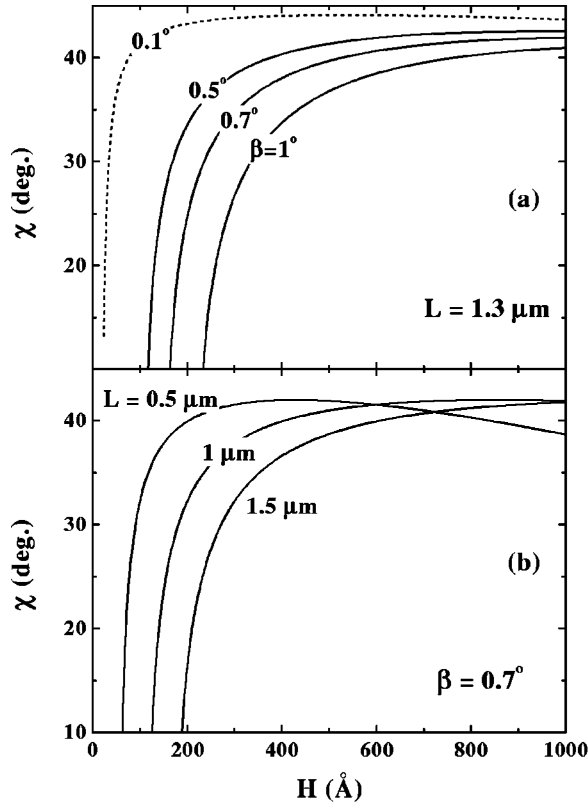

FIG. 6. (a) The obliqueness angle χ as a function of the Si-layer thickness H for different substrate miscut angles β, (b) the obliqueness angle χ for different terrace widths L.

Geometrical reasons for the oblique roughness replication can be ruled out. Let us assume that the shape and evolution of the surface profile are described by the profile function $h(x,t)$. The density of the monolayer steps is thus

$$\rho=\frac{\beta_0-\beta}{h_0}, \quad \text{where} \quad \beta=\frac{\partial h}{\partial x}.$$

The vertical and horizontal components of the step velocity are

$$v_z=\frac{Fh_0\sin(\beta_0)}{\beta_0-\beta}\approx\frac{Fh_0\beta_0}{\beta_0-\beta},$$

$$v_x=\frac{Fh_0\cos(\beta_0)}{\beta_0-\beta}\approx\frac{Fh_0}{\beta_0-\beta}, \tag{13}$$

if we do not take a bunching of steps into account and β_0 is small. During the small time interval dt the surface moves according to $h(x,t+dt)=h(x-v_x dt,t)+v_z dt$. Therefore the evolution of surface profile h does not depend on x,

$$\frac{\partial h}{\partial t}=v_z-\beta v_x=Fh_0=\text{const},$$

which corresponds to a strictly vertical replication direction.

IV. DISCUSSION

The terrace length $L=1.3$ μm was determined from the spacing of the lateral maxima in the RDS stripes in the reciprocal space map presented in Fig. 2 and the angle $\chi=35°\pm10°$ from the obliqueness of the RDS stripes. The theoretically predicted value of χ (about 36° if we assume $\beta=\beta_0$) agrees very well with the experimentally obtained value both as for the absolute value and the direction (see Fig. 6).

The experimental reflectivity data do not indicate that the Si-SiGe interfaces are much smoother than the SiGe-Si interfaces, which is consistent with the findings of Teichert *et al.*[32] Judging from the specular reflectivity, the rms roughnesses of the interfaces $\sigma_{\text{Si-SiGe}}$ and $\sigma_{\text{SiGe-Si}}$ differ only by 1 Å. Atomic force microscopy (AFM) investigations of the surface morphology of the sample, which is capped by a 21 nm thick Si layer, revealed a waviness perpendicular to the direction of the miscut with a period of about 1 μm. We conclude that the buried Si-SiGe interfaces are also not flat. The growth temperature of the Si layers (400 °C) was comparatively low corresponding to a diffusion length of Si adatoms significantly smaller than 1.3 μm, which provides a possible explanation for the nearly undiminished Si-SiGe interface roughness. So far, it is not clear how the surface of the Si layers mimics the SiGe-Si interface profiles during growth. Therefore it cannot be ruled out that the surface morphology influences the obliqueness angle χ to some extent as well.

The height of the step bunches is related to the rms roughness of σ = 7 Å determined by specular x-ray reflection. If we approximate the terrace profile by a sequence of triangles, the rms roughness of a terraced interface is

$$\sigma\approx\frac{h}{\sqrt{12}},$$

which results in a bunch height h of approximately 25 Å. If we assume $\beta=\beta_0$, the step height would be about 100 Å. Both values are obviously too large, since they exceed the thickness of the SiGe layers. Thus the terrace angle β must be much smaller than the nominal miscut β_0, and, in addition, only a part of the measured rms roughness is caused by the terraces. A similar result was found in Holý *et al.*,[22] where nonspecular x-ray reflection from strained $Ga_xIn_{1-x}As/GaAs/GaAs_yP_{1-y}$ superlattices was measured. A terrace angle of $\beta\approx0.3°$ was determined, whereas the nominal miscut angle β_0 was about 2.5°.

The calculated dependence of the skewness angle χ on H for smaller values of β is qualitatively similar. The dashed line in Fig. 6(a) corresponds to $\beta=0.1°$ and $L=1.3$ μm. For $H=180$ Å, which equals the actual thickness of the Si layers, we obtain $\chi\approx42°$. Thus, for sufficiently large values of H, the predicted obliqueness angle χ is rather independent of β. However, for smaller miscut angles the minima and maxima of the inhomogeneous strain fields become shallower and less significant for the growth process.

The measured reciprocal space map of the scattered intensity in Fig. 2 exhibits a distinct asymmetry, the intensity maxima on the right-hand side of the RDS stripes are higher than those on the left side. This asymmetry is caused by the asymmetric profile of the terraced interfaces. The centers of the envelopes of the RDS maxima lie along a line perpendicular to the terrace levels between the step bunches. On the basis of the interface profiles shown in Fig. 3 we simulated

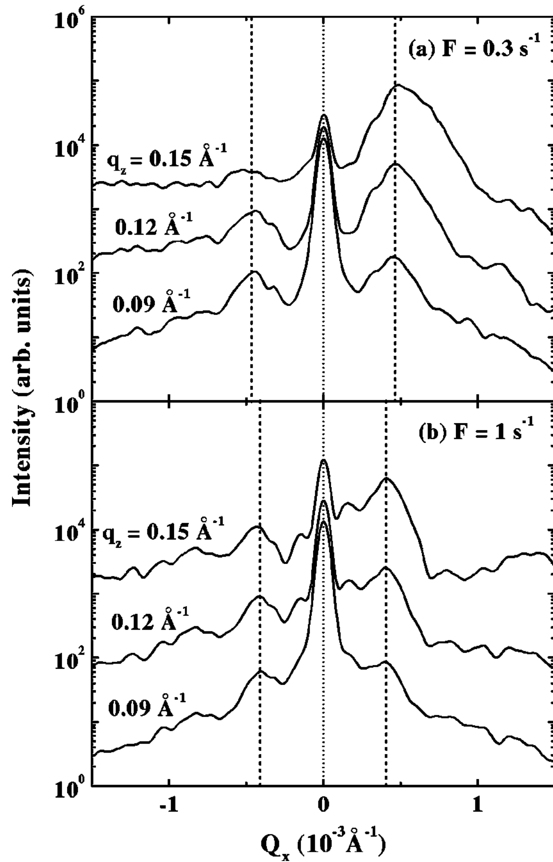

FIG. 7. Simulated Q_x scans through the third, fourth, and fifth superlattice satellite using the interface profiles in Fig. 3 calculated for flux rates of $F = 0.3\ \mathrm{s}^{-1}$ (a) and $F = 1\ \mathrm{s}^{-1}$ (b). The left-right asymmetry of the scattered intensity is much more pronounced for small values of the flux F.

linear Q_x scans of the scattered intensity (Fig. 7). In the case of a small flux F, a strongly asymmetrical interface profile develops, which results in an asymmetric distribution of the scattered intensity in direction parallel to the Q_x axis. In the case of a large flux rate F, the interface profile resembles a wavy structure [see Fig. 3(c)], the monolayer steps are distributed more or less homogeneously and the corresponding x-ray intensity distribution is nearly symmetrical. Therefore a detailed analysis of the reciprocal space distribution of the scattered intensity allows us to determine not only the averaged roughness but also to extract information on the detailed shape of the interfaces.

A localized increase of the in-plane strain $|\epsilon_{xx}|$ in the layer induces the formation of a step bunch. The height of this bunch depends on the absolute value and the width of this strain maximum. If the thickness of the unstrained Si layers increases or if the terrace angle β decreases, the corresponding strain maximum becomes wide and shallow and the number of vertically correlated interfaces is reduced. Hence the correlation of the interfaces breaks down and the angle χ becomes undefined. Naturally, our model for strained multilayers cannot be applied if no misfit strain is present in the structure as is the case for lattice-matched materials.[7]

Apart from the influence of the inhomogeneous strain fields around the step bunches on the oblique replication direction, also stress-driven alloy decomposition may occur during step-flow growth.[31] This mechanism may become important for SiGe layers with higher Ge concentrations than those investigated here and/or for samples with a higher substrate temperature during growth.

In Sec. III B, we have assumed that the terrace edges are straight. If the terrace edges are jagged parallel to the surface, the description of the growth process requires a two-dimensional model (see, e.g., Ref. 8) and the average replication angle χ is expected to decrease. Thus the values of χ in Fig. 6 represent upper limits for the obliqueness angle.

V. SUMMARY

We have presented a quantitative theoretical model for the oblique roughness replication in strained semiconductor multilayers. We have adapted a kinetic step-flow growth model to include effects of inhomogeneous strain due to the formation of step bunches in the strained layers. It turned out that the asymmetric strain distribution in the Si layers above the step bunches is responsible for the oblique roughness replication. The SiGe interface profiles are replicated in the direction of maximum lateral compression, i.e., ''downstairs.'' The predictions of the model are in good agreement with results obtained from measurements of the resonant diffuse x-ray scattering of SiGe/Si multilayers.

ACKNOWLEDGMENTS

This work has been supported by the Grant Agency of the Czech Republic (Project No. 202/97/0003), by the Ministry of Education of the Czech Republic (Project No. VS96102), by the Fonds zur Förderung der Wissenschaftlichen Forschung (Project No. 11557), and by the Bundesministerium für Wissenschaft und Verkehr (Project ''Nanostructures''). We are grateful to J. H. Li for his participation in part of the synchrotron experiments, and one of us (V. H.) acknowledges stimulating discussions with P. Šmilauer (Prague). The experiments have been performed at the OPTICS beamline of the European Synchrotron Radiation Facility (ESRF), and we would like to thank A. Souvorov and A. Freund for their assistance.

[1] Y. H. Xie, D. Monroe, E. A. Fitzgerald, P. J. Silverman, F. A. Thiel, and G. P. Watson, Appl. Phys. Lett. **63**, 2263 (1993).

[2] R. People, J. C. Bean, C. G. Bethea, and L. J. Peticolas, Appl. Phys. Lett. **61**, 1122 (1992).

[3] K. L. Wang and R. P. G. Karunasiri, in *Semiconductor Quantum Wells and Superlattices for Long-Wavelength Infrared Detectors*, edited by M. O. Manasreh (Artech House, Boston, 1993).

[4] P. Kruck, M. Helm, T. Fromherz, G. Bauer, J. F. Nützel, and G. Abstreiter, Appl. Phys. Lett. **69**, 3372 (1996).

[5] T. Kikkawa, T. Makiyama, H. Ochimizu, K. Kasai, and J. Kumeno, J. Cryst. Growth **145**, 799 (1994).

[6] T. Marschner, S. Lutgen, M. Volk, W. Stolz, E. O. Goebel, N. Y.

Jin, and F. Philipp, Superlattices Microstruct. **15**, 183 (1994).
[7] A. A. Wheeler, C. Ratsch, A. Morales, H. M. Cox, and A. Zangwill, Phys. Rev. B **46**, 2428 (1992).
[8] D. Kandel and J. D. Weeks, Phys. Rev. Lett. **74**, 3632 (1995).
[9] J. Tersoff, Y. H. Phang, Z. Zhang, and M. G. Lagally, Phys. Rev. Lett. **75**, 2730 (1995), and the references therein.
[10] D. E. Jones, J. P. Pelz, Y. H. Xie, P. J. Silverman, and G. H. Gilmer, Phys. Rev. Lett. **75**, 1570 (1995).
[11] K. M. Chen, D. E. Jesson, S. J. Pennycook, M. Mostoller, T. Kaplan, T. Thundat, and R. J. Warmack, Phys. Rev. Lett. **75**, 1582 (1995).
[12] C. Roland and G. H. Gilmer, Phys. Rev. B **54**, 2931 (1996).
[13] E. S. Fu, M. D. Johnson, D.-J. Liu, J. D. Weeks, and E. D. Williams, Phys. Rev. Lett. **77**, 1091 (1996).
[14] M. Rost, P. Šmilauer, and J. Krug, Surf. Sci. **369**, 393 (1996), and references therein.
[15] D. E. Savage, J. Kleiner, N. Schimke, Y.-H. Phang, T. Jankowski, J. Jacobs, R. Kariotis, and M. G. Lagally, J. Appl. Phys. **69**, 1411 (1991).
[16] R. L. Headrick and J.-M. Baribeau, J. Vac. Sci. Technol. B **11**, 1514 (1993).
[17] R. L. Headrick and J.-M. Baribeau, Phys. Rev. B **48**, 9174 (1993).
[18] Z. H. Ming, A. Krol, Y. L. Soo, Y. H. Kao, J. S. Park, and K. L. Wang, Phys. Rev. B **47**, 16 373 (1993).
[19] Y. H. Phang, C. Teichert, M. G. Lagally, L. J. Peticolas, J. C. Bean, and E. Kasper, Phys. Rev. B **50**, 14 435 (1994).
[20] R. L. Headrick, J.-M. Baribeau, and Y. E. Strausser, Appl. Phys. Lett. **66**, 96 (1995).
[21] J.-M. Baribeau and D. J. Lockwood, J. Electron. Mater. **24**, 341 (1995).
[22] V. Holý, C. Giannini, L. Tapfer, T. Marschner, and W. Stolz, Phys. Rev. B **55**, 9960 (1997).
[23] V. Holý, A. A. Darhuber, J. Stangl, G. Bauer, J.-F. Nützel, and G. Abstreiter, Nuovo Cimento Vol. **19D**, 419 (1997).
[24] T. S. Kuan and S. S. Iyer, Appl. Phys. Lett. **59**, 2242 (1991).
[25] J. Nützel and G. Abstreiter, Phys. Rev. B **53**, 13 551 (1996).
[26] V. Holý and T. Baumbach, Phys. Rev. B **49**, 10 668 (1994).
[27] D. K. G. de Boer, Phys. Rev. B **53**, 6048 (1996).
[28] V. I. Marchenko and A. Ya Parshin, Zh. Eksp. Teor. Fiz. **79**, 257 (1980) [Sov. Phys. JETP **52**, 129 (1980)].
[29] L. E. Shilkrot and D. J. Srolovitz, Phys. Rev. B **53**, 11 120 (1996).
[30] R. D. Mindlin and D. H. Cheng, J. Appl. Phys. **21**, 926 (1950); **21**, 931 (1950).
[31] J. Tersoff, Phys. Rev. Lett. **77**, 2017 (1996).
[32] C. Teichert, Y. H. Phang, L. J. Petitcolas, J. C. Bean, and M. G. Lagally, in *Surface Diffusion: Atomistic and Collective Processes*, edited by M. C. Tringides (Plenum, New York, 1997), p. 297.